Asia Pacific Academy of Science Pte. Ltd.

Sustainable Social Development 2026, 3(4), 8348.
https://doi.org/10.54517/ssd8348

Article

Flood mapping susceptibility based on Geographic Information Systems (GIS) and the Analytic Hierarchy Process (AHP) method in Bol, Lac Province, Chad, Central Africa

Parfait Altolnan Tombar[1,2,*], Abdou Kailou Djibo[3], Kossi Komi[1], Abdelkerim Ramadan[1], François Teadoum Naringué[1,4], Pierre Bassena[3], Komi Selom Klassou[2]

[1] Regional Centre of Excellence on Sustainable Cities in Africa (CERViDA-DOUNEDON), University of Lome, Lome 01 BP 1515, TOGO
[2] Research Laboratory on the Dynamics of Environments and Societies (LARDYMES), University of Lome, Lome 01 BP 1515, TOGO
[3] African School of Architecture and Urban Planning (EAMAU), Lome 01 BP 2067, TOGO
[4] Research Laboratory on Spaces, Exchange and Human Security (LaREESH), University of Lome, Lome 01 BP 1515, TOGO
*** Corresponding author:** Parfait Altolnan Tombar, ptombar@gmail.com, parfait.tombar@cervida-togo.org

CITATION

Tombar PA, Kailou Djibo AK, Komi K, et al. Flood mapping susceptibility based on Geographic Information Systems (GIS) and the Analytic Hierarchy Process (AHP) method in Bol, Lac Province, Chad, Central Africa. Sustainable Social Development. 2026; 3(4): 8348. https://doi.org/10.54517/ssd8348

ARTICLE INFO

Received: 23 December 2025
Revised: 12 January 2026
Accepted: 20 January 2026
Available online: 6 February 2026

Abstract: Climate change, a major challenge of the 21st century, is increasing the frequency and intensity of urban flooding, particularly in Sahelian cities. In Bol, in the Lac province of Chad, this dynamic has increased the frequency and intensity of flooding, making this risk a recurring threat to the city in recent years. This study aims to map the physical vulnerability (susceptibility) to flooding in the city of Bol using an integrated approach combining remote sensing, geographic information systems (GIS) and the Analytic Hierarchy Process (AHP). Eight key physical factors (precipitation, altitude, slope, land use, distance to watercourses, soil type, drainage density and flow accumulation) were analyzed and weighted using the AHP. The results show that 16.19% of Bol's surface area is highly susceptible to flooding, and 28.08% is highly susceptible, concentrated mainly in low-lying areas and near watercourses. Surveys of 385 households confirm the recurrence of flooding and its significant impact on housing. The map produced is an essential decision-making tool for communities, decision-makers and urban stakeholders in planning actions to reduce current and future flood risks in the city of Bol. However, the lack of quantitative validation of the model is a methodological limitation, opening the door to future research incorporating uncertainty and exposure analyses.

Keywords: flood vulnerability; Geographic Information System (GIS); Analytic Hierarchy Process (AHP); remote sensing; Bol; lake (chad)

1. Introduction

Climate change is no longer an unfamiliar term [1]. Today, it is one of the greatest challenges facing humanity, as it increases the frequency and intensity of extreme events such as droughts, floods, etc. [2–4]. On a global scale, these hydrometeorological phenomena cause significant human losses, considerable material damage and lasting degradation of socio-economic systems, particularly affecting urban infrastructure and housing [3,5]. These findings show that communities around the world are becoming increasingly vulnerable to natural disasters and climate change, and according to the World Bank, approximately 50% of the world's population lives in areas exposed to natural hazards [6].

Floods, characterised by the submersion of normally dry areas, are one such risk [7]. They are among the most frequent and devastating climate hazards worldwide [8,9]. Between 1998 and 2017, they affected more than 2 billion people [10], with a notable increase in their frequency and intensity in tropical and Sahelian regions. In

Central and West Africa, the floods of 2024 caused massive destruction of housing (300,000 homes), forced the displacement of millions of people, and significantly worsened living conditions, revealing the high vulnerability of cities to flooding [11]. Chad, regularly ranked among the countries most vulnerable to climate change [12], is a prime example of this situation, with major floods in recent years affecting the population and prompting the Chadian government to declare a national state of emergency in 2022 [13].

In this national context, the town of Bol, located on the southern shore of Lake Chad, is a particularly relevant case study. Its location in a low-lying plain, dominated by hydromorphic and alluvial soils, promotes water stagnation during the rainy season [14]. The lake, which recedes or overflows depending on the season, causes recurrent flooding that affects the riparian areas. This physical vulnerability is exacerbated by sustained population growth, the arrival of displaced populations, and rapid, unplanned urbanisation, which has led to the occupation of low-lying, flood-prone areas [14–16]. Recurrent flooding in Lac Province, particularly in 2024, affected 102,145 households, left 71,070 people homeless, led to the destruction of 72,586 homes and 76,712 hectares of crops, caused the loss of 51,686 head of livestock and resulted in 43 deaths [17], highlighting the urgent need for decision-making tools adapted to the local context.

Conceptually, it is essential to clearly distinguish between flood hazard, vulnerability and risk. Flood risk is generally defined as the result of the combination of hazard, exposure and vulnerability. This study focuses specifically on assessing physical vulnerability, also referred to as flood susceptibility, understood as the intrinsic propensity of an area to be affected by flooding based on its hydro-geomorphological, pedological and environmental characteristics. This methodological choice is motivated by the availability of spatial data and the need to produce operational mapping at the urban scale, while recognising that exposure and adaptive capacity are complementary dimensions of overall risk.

Hazard mapping is an essential risk management tool, enabling the identification of areas likely to be exposed to various types of hazards, the planning of mitigation and adaptation measures, and the improvement of disaster preparedness, response and recovery [18]. There is no longer any doubt about the need for decision-making tools to assess a city's flood susceptibility. Numerous studies have shown that remote sensing and geographic information systems (GIS) can be combined to map flood risk [7]. Remote sensing is useful for obtaining high-resolution images of flooded areas [19,20]. However, optical imaging has its limitations in detecting flooded areas when they are covered by dense vegetation or when the sky is very cloudy at the time of flooding [21,22]. These limitations compromise the accuracy of observation and mapping of affected areas [22]. The integration of remote sensing data into GIS is the most widely used method for mapping flood risks [7]. Numerous studies worldwide have used a combination of GIS methods and multi-criteria decision analysis (MCDA) to characterise flood hazards with high accuracy [18,7,23,24]. Among MCDA methods, the Analytic Hierarchy Process (AHP) has proven effective in mapping flood vulnerability [7,25]. AHP is a decision-making framework that helps prioritise and select the best option by breaking down a complex decision into a hierarchy of objectives, criteria and alternatives [26]. The AHP method improves decision-making

by providing clearer visualisation and enhanced mapping capabilities, thereby facilitating the development of hazard maps [18].

Previous studies, such as those in [7], have combined remote sensing data, GIS methods, and the Analytic Hierarchy Process (AHP) to map flood susceptibility in peri-urban areas of Greater Lomé, Togo. Kazakis et al. [27] used a multi-criteria methodology in the Rhodope–Evros region of Greece to identify flood-prone areas at the regional scale, combining spatial data in a GIS environment with the Analytic Hierarchy Process (AHP). And Sajid et al. [18] assessed the combined risks of flooding and landslides in the Kohistan district of northern Pakistan, a mountainous region highly vulnerable to natural hazards, using an integrated approach combining GIS, AHP and remote sensing. Their results show that 77% of the district is at high risk of flooding, while 30.5% is at high risk of landslides. Nevertheless, this work also highlights the highly contextual nature of the results, which depend on the factors selected, the weightings assigned and local hydro-geomorphological specificities. Consequently, the direct transposition of models from one territory to another remains limited and requires methodological adaptations.

In the context of Chad, research on flooding has mainly focused on socio-economic impacts, adaptation strategies or work in certain large cities, particularly N'Djamena [28–30]. In Bol, existing work on vulnerability to climate risks has mainly focused on the agricultural, fishing and pastoral sectors, as well as on cross-cutting issues such as migration and gender, leaving little room for analysis of urban vulnerability to flooding [12,31–33]. To our knowledge, no study has yet proposed an integrated flood susceptibility map combining remote sensing data, GIS analysis, the AHP method and field surveys at the scale of the city of Bol.

Considering these findings, this study aims to fill a scientific and operational gap by advancing traditional flood-mapping approaches based on GIS and the Analytic Hierarchy Process (AHP). Unlike previous studies, which were often limited to purely physical modelling and large-scale analyses, this research adopts a broader methodological approach combining remote sensing data, GIS analysis, AHP and georeferenced field surveys, enabling the results of the susceptibility model to be compared with empirical observations from affected households. The analysis is conducted at the fine scale of a secondary Sahelian city, Bol, with homogeneous spatial resolution, highlighting intra-urban heterogeneities that have been little explored in previous GIS-AHP studies. Finally, the explicit linking of the susceptibility map with the built-up area and the distribution of affected households makes the study highly relevant for decision-making, providing a tool that can be directly used for urban planning, risk management and the orientation of local adaptation strategies.

The study focuses on the following research question: How do physical factors interact to shape the spatial distribution of flood susceptibility in the city of Bol? The main objective is to map physical flood susceptibility using an integrated GIS-AHP approach. More specifically, the study seeks to: (i) analyse local populations' perceptions of rainfall and flood recurrence; (ii) prioritise the physical factors contributing to flood vulnerability using the Analytic Hierarchy Process; and (iii) produce a susceptibility map to support urban planning, risk management and the development of local adaptation strategies in the city of Bol.

2. Materials and methods

2.1. Study area

This study is being conducted in the town of Bol, located on the shores of Lake Chad, 153 km north of the capital, in the Sahelian zone of Chad, between 13°27'31" north latitude and 14°42'53" east longitude (**Figure 1**). The town of Bol is strategically located because it borders Nigeria, Niger, and Cameroon. It also benefits from an arid climate and a large surface water basin known as the "arm of Lake Chad", an endorheic lake [12,34]. It is also located on a plain of hydromorphic soils, including lacustrine alluvial soils, sandy-clay soils, alluvial soils, sandy-beige to sandy-clay soils and tropical black clays [14]. The city is located within a very active trade network, distinguished by an economy based mainly on primary sector activities, where its economic importance is reinforced by substantial agricultural production from the Lake Chad polders [16].

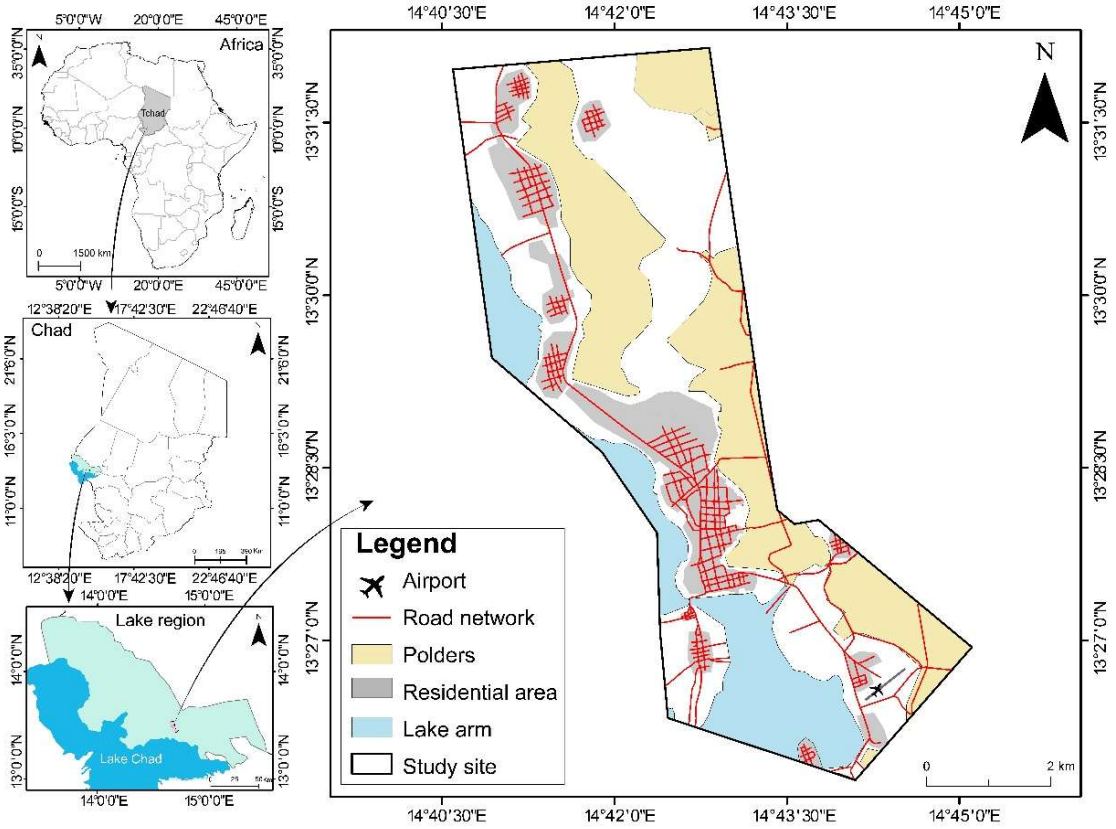

Figure 1. Geographical location of the study area.

Figure 2 shows the ombrothermic curve for the city of Bol and highlights a highly contrasting climate seasonality. The dry season, particularly marked from January to March, is characterised by almost total rainfall absence (0 mm), while the rainy season lasts from May to September, with maximum rainfall in August (136 mm). Temperatures peak in May (44.6 °C) before the rains set in, while average monthly temperatures range from 23.4 °C in January to 34.3 °C in May.

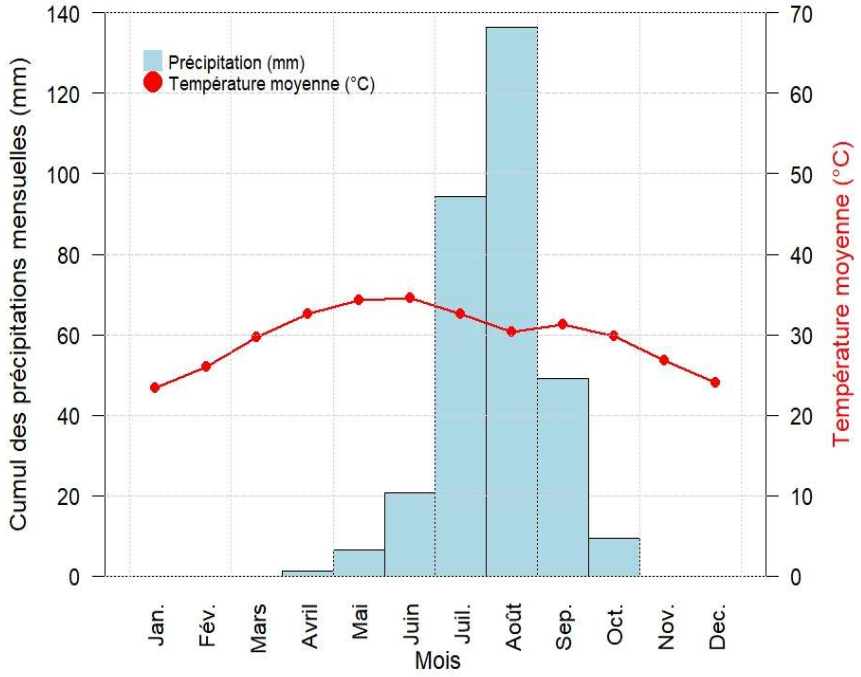

Figure 2. Ombrothermic diagram of the city of Bol, based on average monthly temperature and precipitation data from 1982 to 2022. Source: Synoptic data collected from the national meteorological agency (ANAM), 2024.

2.2. Data used

Table 1 shows all the data used in this study, which comes from remote sensing products and fieldwork.

Table 1. The various data used in this study.

Data type	Descriptions	Sources
Digital elevation model	Field-corrected radiometric data	https://www.earthdata.nasa.gov/data/projects/alos-palsar-rtc-project (accessed on 14 July 2025)
Sentinel-2 image	Land use and land cover data for the year 2024	https://livingatlas.arcgis.com/landcoverexplorer/#mapCenter=14.48797%2C13.40043%2C10.71&mode=step&timeExtent=2017%2C2021&year=2024 (accessed on 15 July 2025)
Soil data	Soil Grids soil map developed by ISRIC-World Soil Information	https://soilgrids.org/ (accessed on 17 September 2025)
Rainfall data	Continental-scale daily rainfall estimates for 2001-2024 from the Famine Early Warning Systems Network project	https://power.larc.nasa.gov/data-access-viewer/ (accessed on 22 July 2025)
Data on the 2024 floods	Field data on households affected by the 2024 floods	Fieldwork in 2024

2.3. Selection of criteria

The criteria were selected based on their contribution to the genesis of flooding in the study area and on their recurrent use in previous scientific literature employing the same methods. **Table 2** summarises the main previous studies cited as references.

Table 2. Summary of previous studies using the same method.

Parameters	Number of criteria	Methods	Study area	References
Altitude, slope, distance to a watercourse, rainfall intensity, accumulation flow, land cover/land use, soil type.	7	AHP, GIS, Remote Sensing	Grand Lomé (Togo)	Blakime et al., 2024 [7]
Slope, curvature, land cover/land use, altitude, distance to a watercourse, soil type, Normalised Difference Vegetation Index (NDVI), precipitation, Topographic Wetness Index (TWI).	9	AHP, GIS, Remote Sensing	Kohistan (Pakistan)	Sajid et al., 2025 [18]
Slope, drainage density, soil type, isohyet, population density, land cover/land use and sewerage system density.	6	AHP, GIS, Remote Sensing	Abidjan (Côte d'ivoire)	Danumah et al., 2016 [35]
Altitude, slope, surface curvature, Topographic Wetness Index (TWI), Stream Power Index (SPI), precipitation, depressions, drainage density, and distance to a watercourse.	9	AHP, GIS, Remote Sensing	Sud-Ouest de l'Arabie Saoudite	Alarifi et al., 2022 [24]
Precipitation, distance to a watercourse, altitude, slope, land cover/land use, drainage density, soil type, lithology.	8	AHP, GIS, Remote Sensing	Bassin de Shatt Al-Arab (Iraq-Iran)	Allafta et al, 2021 [24]
Land cover/land use, altitude, slope, surface runoff, distance to a watercourse, precipitation, soil texture, soil drainage, and relief.	9	AHP, Weighted Linear Combination (WLC), GIS, Remote Sensing	Bassin de Kemp-Welch (Papouasie-Nouvelle-Guinée)	Morea et al., 2020 [25]
Elevation, slope, drainage density, distance to a watercourse, topographic Wetness index (TWI), modified normalised water index, precipitation, normalised difference vegetation index (NDVI), and lithology.	9	AHP, GIS, Remote Sensing	Bassin versant de Cheliff-Ghrib (Algérie)	Mokhtari et al., 2023 [26]
Precipitation, slope, flow accumulation, elevation, distance to watercourse, land cover/land use, soil type.	7	AHP, GIS, Remote Sensing	Rhodope-Evros (Grèce)	Kazakis et al., 2015 [27]
Precipitation, normalised difference vegetation index, drainage density, flow accumulation, topographic moisture index, elevation, slope, curvature, distance to watercourse, soil type, land use/land cover.	11	AHP, GIS, Remote Sensing	District de Dega Damot, (Éthiopie)	Negese et al., 2022 [36]
Precipitation, slope, land use/ land cover, drainage density, distance to road, topographic Wetness index, distance to watercourse, normalised difference vegetation index, and altitude.	9	AHP, GIS, Remote Sensing	Freetown (Sierra Leone)	Koroma et al., 2024 [37]
Altitude, slope, normalised differential vegetation index (NDVI), land use/land cover, soil type, drainage density, distance to road, distance to watercourse, precipitation, topographic Wetness index (TWI).	10	AHP, GIS, Remote Sensing	Comté de Davidson (Etats-Unis)	Shrestha et al., 2025 [38]
Flow accumulation, slope, distance to a watercourse, drainage network density, land use/ land cover, precipitation, and permeability.	7	AHP, GIS, Remote Sensing	Dades Wadi (Maroc)	Aichi et al., 2024 [39]
Flow accumulation, distance to a watercourse, drainage network density, precipitation, slope, land use/ land cover, and permeability.	7	AHP, GIS, Remote Sensing	Taguenit Wadi (Maroc)	Ikirri et al., 2022 [40]

Following a review of the literature on flood mapping studies using GIS approaches and the Analytic Hierarchy Process (AHP), supplemented by an analysis of specific studies in the study area, observations from fieldwork, and consideration of data availability and quality, eight (8) physical factors determining the genesis of floods were selected and ranked. These factors were chosen for their documented role

in flood dynamics and their relevance to the city of Bol's hydro-geomorphological context.

Rainfall intensity is the most influential factor in this study, carrying the highest weight in the flood susceptibility analysis. Floods are intrinsically linked to rainfall, whose intensity and duration directly determine the volume of water generated, surface runoff and soil saturation [36,41]. Regions receiving heavy rainfall are therefore more prone to flooding than those with low rainfall [37]. In the context of Bol, which is characterised by highly seasonal rainfall, this factor plays a central role in flooding.

Altitude appears to be the second most important factor. Low-lying areas are generally more vulnerable because they receive and accumulate runoff from higher areas [24,42]. As the city of Bol is located on a low-lying plain, slight variations in altitude are sufficient to cause water stagnation and the spatial expansion of flooded areas, underscoring the importance of this parameter.

The terrain slope ranks third among the factors analysed. It directly influences runoff and infiltration processes. Areas with gentle slopes promote water accumulation and stagnation, thereby increasing susceptibility to flooding, while steeper slopes induce rapid runoff that can lead to flash floods and locally more destructive flooding [39,40,43]. In the Bol plain, characterised by very gentle slopes, this factor significantly contributes to flood risk.

The fourth factor for mapping flood susceptibility is land use and land cover (LULC). These contribute to flooding by influencing infiltration and runoff. Urbanised areas limit infiltration and increase runoff, thereby increasing the risk of flooding [38]. Conversely, dense vegetation cover promotes infiltration and reduces this risk [36,40]. In the Sahelian context, as in Bol, populations attribute flooding to land-use changes [44], confirming that LULC is an important physical factor in identifying vulnerable areas [7].

Distance from waterways is also considered the fourth factor in flood risk assessment, as areas located near the hydrographic network act as floodplains during heavy rainfall and are therefore the most vulnerable, while the danger decreases with distance [38,41]. Several studies show that populations living near watercourses are particularly exposed to flooding and overflowing [40,43], a situation frequently observed in the low-lying neighbourhoods of Bol.

Soil type plays an important role in flood dynamics due to its physical properties, such as texture, permeability, and structure, which directly influence drainage, infiltration, and surface runoff [45]. The hydromorphic and low-permeability soils in Bol limit infiltration and promote water stagnation, thereby increasing the risk of flooding.

The density of the drainage network is also considered in assessing physical vulnerability to flooding, as it directly influences runoff, flow rates and erosion potential. Areas with high drainage density quickly concentrate runoff and are often more prone to flooding, particularly during heavy rainfall [38]. In Bol, the natural and artificial drainage network significantly affects the spread of water during high-water periods.

Finally, flow accumulation is also a relevant criterion in identifying flood-prone areas. This parameter has often been used in numerous previous studies [36,42]. It

represents the volume of water drained from upstream cells into a given cell, thereby influencing flow concentration and flood risk [40], particularly in low-slope areas such as Bol.

2.4. Methods

Several types of data and different methodologies were used in this study. On the one hand, an analytical approach based on physical factors was used to map flood susceptibility, structured in seven main steps: (i) data collection and preparation (precipitation, DTM, land use, soils, hydrography); (ii) harmonisation of data within a single coordinate system and division of the study area; (iii) derivation of topographical and hydrological variables (slope, flow accumulation, drainage density, distance to watercourses); (iv) normalisation/reclassification of each factor into ordinal susceptibility classes; (v) estimation of weights using the Analytic Hierarchy Process (AHP); (vi) weighted linear combination (WLC) to produce the susceptibility index and map; (vii) validation by comparison with field data and spatial consistency analysis of affected households. In addition, a quantitative approach using questionnaires administered to households was used to gather information on households' perceptions of flooding.

2.4.1. Methodology for developing the flood susceptibility map

The flood susceptibility map was developed by integrating remote sensing data and geographic information systems (GIS) and applying the AHP approach [7,40]. The hydro-geo-morpho-climatic data layers, namely land use and land cover, distance from watercourses, precipitation, drainage network density, soil infiltration rate, flow accumulation, slope and altitude, were generated using GIS and remote sensing techniques from spatial data collected from various sources.

Preparation of data relating to flood factors

In this study, eight (8) determinants of flood risk were selected based on the specific characteristics of the study area, data availability, and previous studies on flood risk [7,23,39,40,42]. These factors include precipitation, altitude, slope, land use and land cover, distance from watercourses, soil infiltration rate, drainage network density and flow accumulation. In this study, the precipitation index was chosen to represent precipitation in the study area, and it was calculated using the Modified Fournier Index (MFI) with Equation (1) [7,41]:

$$\mathrm{MFI} = \sum_{i=1}^{12} \frac{P_i^2}{P} \tag{1}$$

where FMI is the Modified Fournier Index, i is the month, P_i is the monthly average rainfall (mm), and P is the average annual rainfall (mm).

To map rainfall, daily precipitation data from 2001 to 2024 were downloaded from the POWER (Prediction of Worldwide Energy Resources) project database, a NASA (Langley Research Centre) initiative that makes ready-to-use meteorological data accessible [46]. This data was imported and processed using QGIS software (version 3.34.12). Land use and land cover (LULC) information was extracted from Sentinel-2 images using supervised classification with QGIS software (version 3.34.12), while the soil type map was generated by classifying the soil type layers of

the Harmonised Global Soil Data (HGS) provided by Soil Grids, a global digital soil mapping system developed by ISRIC-World Soil Information, using QGIS software (version 3.34.12) [47]. The elevation and slope maps were derived from the Digital Terrain Model (DTM) of the study area, while the flow accumulation map was generated after filling in the DTM map of the study area to create the flow direction map from the Digital Terrain Model (DTM) using QGIS software. The distance-to-watercourse map was generated using the buffer tool in the GIS environment, accounting for existing hydrographic networks. Areas within 200 m of the hydrographic network were considered particularly vulnerable to flooding, in line with previous studies [7,48].

It should be noted that the maps of the eight (8) flood hazard factors were reclassified to the same scale, ranging from 1 (very low) to 5 (very high), and then resampled to a 10 m spatial resolution. The factor classes, including distance to the hydrographic network, altitude, and precipitation, were generated using the natural breaks method, as in previous studies, because it is useful for assigning labels to an ordinary scale [7,49]. Land use and land cover (LULC) classes were obtained from [50], while slope and soil infiltration rate classes were estimated as suggested by [51,52], respectively. Due to the diversity of data spatial resolutions used in this study, a resampling process was applied to harmonise the image resolutions from different sources. This step, which is essential in the processing of spatial data, ensures the consistency and homogeneity of information, which is a prerequisite for reliable and comparable analyses. The bilinear method was chosen for resampling because it preserves visual continuity while ensuring smooth data integration. It estimates the value of new pixels by calculating a weighted average of their neighbouring pixels, which provides more consistent and accurate results when harmonising spatial resolutions.

The Digital Terrain Model (10 m) resolution was used as a reference to adjust the resolutions of the other images. The 10 m spatial resolution was chosen to address heterogeneity in data resolution, which required standardisation to ensure consistent integration into the multi-criteria analysis. This resolution is particularly suited to the analysis of intra-urban heterogeneities in the city of Bol, where slight topographical variations cause water stagnation. It is also consistent with the resolution of the main spatial data used. Continuous variables were resampled using bilinear interpolation, while categorical variables were processed using the nearest neighbour method to limit spatial bias.

Use of the AHP method

Given that the various flood factors do not have equal importance in the flood generation process, Saaty's Hierarchical Analysis Method (AHP) was applied to estimate the relative weights of each factor [7,53]. This multi-criterion decision-making method, based on pairwise comparison matrices, enables the determination of the relative importance of each criterion and the selection of the most relevant options [53]. This decision-making method has the advantage of incorporating a consistency test, thereby reducing uncertainty in the weighting process, which explains its use in several previous studies [7,39,40,42]. The relative importance of the criteria is estimated on a scale of 1 to 9, from 1 (least important) to 9 (most important) (**Table**

3).

As part of this study, a panel of five experts was assembled, comprising specialists in GIS/remote sensing, hydrology/hydraulics, geomorphology/paedology, urban planning/risk management, and architecture/urban planning, with an average of 5 years of professional experience. Each expert completed a pairwise comparison matrix on the Saaty scale (1–9). The individual matrices were aggregated by geometric mean to obtain a consensus matrix, in accordance with AHP methodological recommendations. The final weights were calculated from the principal eigenvector and normalised to sum to 1.

Table 3. Importance scales used in the pairwise comparison matrix [7,54].

Intensity of importance	Definition	Description
1	Equal importance	Two criteria contribute equally to the objective
3	Moderate importance	Experience and judgement favour one slightly over the other
5	High importance	Experience and judgement strongly favour one over the other
7	Very high importance	Experience and judgement strongly favour one criterion over another
9	Extreme importance	The evidence in favour of one criterion over another is of the highest possible validity.
2,4,6,8	Intermediate values	When agreement is necessary.

To calculate the weights of each parameter, AHP begins by creating a pairwise comparison matrix ($M = (B_{ij})$) [7,54]. Each numerical value of M represents the relative importance of parameter i compared to parameter j. If $B_{ij} > 1$, parameter i is more important than parameter j, while if $B_{ij} < 1$, parameter i is less important than parameter j. If both parameters have the same importance, then $B_{ij} = 1$. The mathematical values satisfy the condition given in Equation (2):

$$B_{ij} \times B_{ji} = 1 \tag{2}$$

After developing the comparison matrix and defining the weights of the factors, the Consistency Ratio (CR) was calculated according to Equation (3) proposed by [54]:

$$\mathrm{CR} = \frac{\mathrm{CI}}{\mathrm{RI}} \tag{3}$$

where CI is the Consistency Index, and RI is the Random Index, whose value depends on n, which is the number of criteria (factors). The value of the Consistency Index (CI) was obtained using Equation (4):

$$I = \frac{\lambda_{max} - n}{n - 1} \tag{4}$$

where λ max represents the largest eigenvalue of the matrix and n represents the number of parameters. The Random Index (RI) constant depends on n (**Table 4**). When RC < 0.1, the assessment is consistent and reliable results can be expected from the AHP model.

Table 4. Random index for calculating the consistency rate [7,54].

N	**1**	**2**	**3**	**4**	**5**	**6**	**7**	**8**	**9**	**10**	**11**	**12**	**13**
IA	0	0	0,58	0,90	1,12	1,24	1,32	1,41	1,45	1,49	1,51	1,48	1,56

Development of the flood susceptibility index model

The Flood Hazard Index (FHI) model proposed in this study accounted for eight (8) factors: precipitation, altitude, slope, land use and land cover, distance to watercourses, soil infiltration rate, drainage network density, and flow accumulation. Based on the estimated weights of these different factors and their scores (**Table 4**), the Flood Risk Index for each pixel (FHIj) was calculated using Equation (5) [7]:

$$\mathrm{FHI} = \sum W_J \times X_j \tag{5}$$

where XJ is the ranking score of each class relative to layer *J*, and WJ is the weight of layer *J*. In addition, the Inflation Risk Index (FHI) has been divided into five (5) classes, namely: very low, low, moderate, high and very high.

Relationship between the flood susceptibility map, data from the 2024 field surveys, and the built-up area of the city of Bol

In this study, the relationship between the flood susceptibility map, field survey data collected in 2024, and the built-up area of the city of Bol was established using an approach like that employed in previous studies [56,57]. This involved using field data collected with GPS during surveys conducted in Bol in 2024, as well as mapping the city's built-up areas using shapefile data from the municipality of Bol's Geographic Information System (GIS) department. The two maps produced from this data were then superimposed on the flood susceptibility map, developed using GIS and the AHP method, to analyse the spatial relationships between the flood zones identified by the AHP model, the built-up area of the town of Bol, and the distribution of households observed in the field.

Figure 3 presents the entire flowchart, illustrating the processes used to map flood risks in this study.

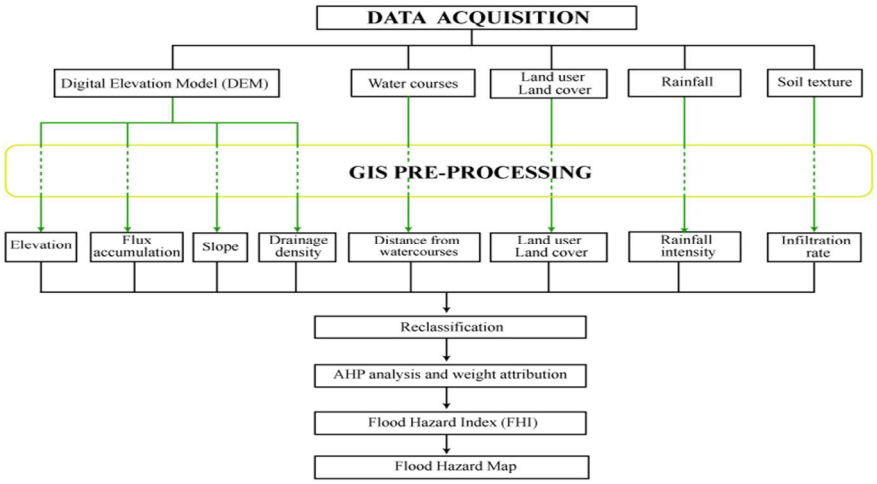

Figure 3. Flowchart of the methodology used to map flood susceptibility in the city of Bol.

Uncertainty and sensitivity

The weighting of factors using the Analytic Hierarchy Process (AHP) and the reclassification thresholds introduce uncertainty into the assessment of flood susceptibility, particularly in transition zones between classes. Due to insufficient data to conduct a formal uncertainty or sensitivity analysis, this dimension is recognised as a methodological limitation of the study. Nevertheless, it constitutes an important research perspective, particularly through the implementation of systematic sensitivity analyses, variants of fuzzy AHP, or hybrid approaches combining multi-criteria methods and statistical or machine learning models.

2.4.2. Household survey

The household surveys covered a sample of 385 people from different socio-professional categories in 2024 in the city of Bol, with households randomly selected to avoid duplication. The questionnaires were created using Kobo Toolbox and administered using the Kobo Collect application, version 2023.2.4 [12]. The heads of each household were considered as samples. This approach has already been used in recent studies conducted in Central Africa [58]. In the field, vernacular was used for those who did not understand the interview language. We also used translators and local informants to translate and explain the interview to city dwellers. To do this, verbal consent was obtained from respondents before each interview began. These surveys collected information on the floods that occurred in the city of Bol in 2024.

The survey used a questionnaire combining closed-ended and open-ended questions, a methodological approach also used in previous studies in Central Africa [58]. The data collected from households covers the following variables:

- Socio-economic characteristics of respondents (gender, age, education level, occupation, household income);
- Households' perceptions of flooding;
- Identify households affected by the 2024 floods.

To determine the sample size, the inverse of the margin-of-error Equation (6) proposed by Daniel Schwartz was used. Let n be the sample size for a rounding of q, and we have the following:

$$n_q = \frac{[(z_a)^2 \, x \, P(1-P)]}{d^2} \tag{6}$$

With Za: Fixed margin or margin reduced to a 5% risk (1.96), which corresponds to a 95% confidence interval; *d*: margin of error set at 3% and *P*: proportion of the population of the town of Bol in the Lake Chad region (8.29%, or 0.0829 rounded to 0.1).

By using the digital application:

$$n_q = \frac{[(1{,}96)^2 \, x \, 0{,}1(1-0{,}1)]}{(3\%)^2}$$

n_q =385

2.4. Data analysis and processing

Spatial data were processed and analysed using QGIS 3.34.12, a Geographic

Information System, to integrate, structure, and exploit all the geographic data used in this study. The maps produced were then harmonised and finalised in Adobe Illustrator 2024 to improve their readability and graphic quality. For the analysis of socio-demographic and professional data and perceptions related to flooding, respondents' answers from the Kobo Toolbox platform were exported as CSV files and imported into Excel. The processing included cleaning the databases (detecting and managing missing values, checking consistency, recoding and formatting variables). The Microsoft Office suite was also used to organise, structure and format the additional data tables. Additional validation was carried out by analysing the spatial distribution of households affected by flooding according to susceptibility classes. A χ^2 goodness-of-fit test was used to assess whether the affected households were significantly concentrated in the moderate-to-high susceptibility classes.

3. Results

3.1. Responses from household survey participants

3.1.1. Profiles of household survey respondents

The results show (**Table 5**) a strong male predominance among respondents (87.01%) and a population predominantly of working age (85.46% aged 20 to 59). Analysis of place of birth shows that 61.56% of respondents are native to Bol and 23.12% to Lac province, indicating a predominantly indigenous population. The level of education is heterogeneous, with a high proportion of households with no formal education or from Koranic schools (53.77%), although a quarter of respondents have a university degree (26.49%). The dominant activities are trade (31.43%) and agro-pastoral and fishing activities (30.13%), both of which are highly sensitive to climate hazards. Finally, more than half of households (52.21%) have monthly incomes of less than 100,000 CFA francs.

Table 5. Information on participants in the household survey.

Information	Category	Frequency	Percentage (%)
Gender	Male	335	87.01
	Female	50	12.99
Age group	Under 20 years old	13	3.38
	20 to 39 years old	196	50.91
	40 to 59 years old	133	34.55
	60 years old and over	43	11.17
Place of birth	Bol	237	61.56
	Lac Province	89	23.12
	Chad	43	11.17
	Outside Chad	16	4.15
Level of education	None	93	24.16
	Koranic school	114	29.61
	Primary education	31	8.05
	Secondary education	45	11.69

Table 5. (*Continued*).

Information	Category	Frequency	Percentage (%)
Level of education	University education	102	26.49
Occupation	Farmer/fisherman/agricultural worker	116	30.13
	Craftsman	14	3.64
	Private sector employee	56	14.55
	Public sector employee	39	10.13
	Retired	9	2.34
	Trader	121	31.43
	Student	12	3.12
	Unemployed	14	3.64
	Other	4	1.04
Monthly income	Less than 59,999 CFA francs	118	30.65
	60,000-99,999 CFA francs	83	21.56
	100,000-199,999 CFA francs	98	25.45
	200,000 CFA francs and above	86	22.34

3.1.2. Perception of rainfall and flood recurrence in the city of Bol by the population

The results presented in **Table 6** highlight households' perceptions of rainfall regularity and intensity, flooding frequency, accessibility of residential areas, presence of rainwater drainage systems, and their experience of the 2024 floods in the city of Bol. The results show that 70.91% of respondents consider rainfall regular, while 29.09% consider it irregular. Regarding its intensity, 58.70% of respondents describe it as heavy, 30.39% as moderate, and 10.91% as light. Furthermore, 63.90% reported having been affected by the 2024 floods, compared to 36.10% who were not. And 38.70% reported losing their homes, while 61.30% reported not losing them. As for the frequency of flooding, 49.87% of respondents perceived it as annual, while 31.43% said it occurred every 1 to 5 years, 16.62% every 6 to 10 years and only 2.08% every 10 years or more. The results regarding the accessibility of residential areas during the rainy season show that most households (47.53%) face difficult-to-very difficult access conditions (37.66% difficult and 9.87% very difficult). Only 20.52% of households report easy accessibility, and 31.95% report passable access conditions. Furthermore, analysis of drainage or rainwater retention structures reveals a marked lack of hydraulic infrastructure, with 94.03% of households reporting the absence of such structures in their residential areas. Only 5.97% of respondents benefit from drainage systems.

Table 6. Responses from participants in the household survey on perceptions of rainfall and the recurrence of flooding in the city of Bol.

Variables	Answers	Frequency	Percentage (%)
Precipitation regularity	Yes	273	70.91
	No	112	29.09

Table 6. (*Continued*).

Variables	Answers	Frequency	Percentage (%)
Rainfall intensity	Strong	226	58.70
	Medium	117	30.39
	Weak	42	10.91
Impact of the 2024 floods	Yes	246	63.90
	No	139	36.10
Destroyed houses	Yes	149	38.70
	No	236	61.30
Flood frequency	Every year	192	49.87
	1 to 5 years	121	31.43
	6 to 10 years	64	16.62
	Over 10 years	08	2.08
Accessibility of the residential area during the rainy season	Easy	79	20.52
	Fair	123	31.95
	Difficult	145	37.66
	Very difficult	38	9.87
Existence of drainage or rainwater retention structures in their area	Yes	23	5.97
	No	362	94.03

3.2. Flood risks in the town of Bol

3.2.1. Physical factors contributing to flood risk in the town of Bol

The classes, ratings and surface coverage of the eight (8) flood risk factors (precipitation, altitude, slope, land use and cover, distance from watercourses, soil infiltration rate, drainage network density, and flow accumulation) were combined to identify the most exposed areas. The results of this compilation are presented in **Table 7**.

Table 7. Physical factors contributing to flood risk in the study area.

Factors	Class	Notation	Area coverage	
			Ha	Percentage (%)
Rainfall intensity (mm)	38–64	1	3.52	0.08
	65–82	2	960.02	23.09
	83–96	3	251.47	6.05
	97–118	4	2284.39	54.93
	119–157	5	659.15	15.85
Elévation/Altitude (m)	275–280	5	903.21	21.72
	280–285	4	1112.76	26.76
	285–290	3	688.44	16.55
	290–295	2	1175.51	28.27
	295–304	1	278.63	6.70

Table 7. (*Continued*).

Factors	Class	Notation	Area coverage	
			Ha	Percentage (%)
Slope (%)	0–0,5	5	1361.66	37.74
	0,5–1	4	982.20	23.62
	1–2	3	1365.86	32.84
	2–3	2	433.82	10.43
	3–4	1	15.02	0.36
Land use and land cover (pixels)	Water	5	603.14	14.50
	Built	4	749.30	18.02
	Bare soil	3	2244.20	53.97
	Crop	2	282.33	6.79
	Vegetation	1	279.58	6.72
Distance from the hydrographic network (m)	<200	5	552.99	13.30
	200–500	4	844.47	20.31
	501–1000	3	1495.99	35.97
	1001–2000	2	1231.29	29.61
	>2000	1	33.81	0.81
Soil (infiltration rate, mm/h)	Clayey	5	661.54	15.91
	Alluvial and hydromorphic	4	16.02	0.38
	Sandy	3	2201.89	52.95
	Ferralitic/leached	2	1184.44	28.48
	Poorly developed	1	94.66	2.28
Drainage density (m/m^2)	1–4	1	2487.35	59.81
	4–10	2	874.23	21.02
	10–16	3	582.42	14.01
	16–23	4	177.49	4.27
	23–34	5	37.07	0.89
Flow accumulation (pixels)	0–101	1	3990.56	95.96
	102–303	2	64.17	1.54
	304–551	3	19.28	0.46
	552–1135	4	54.34	1.31
	1136–2866	5	30.20	0.73

The spatial distribution of various rainfall intensity classes (**Figure 4**; **Table 7**) indicates that the highest values (97–118 mm) cover more than half of the study area (54.94%), particularly around Bol, Tandal, and Berim. Conversely, locations in the north and northwest, such as Matafo 1, Matafo 3 East, Matafo 3 West, and Katchikitchiri, experience lower rainfall, while intermediate areas like Marafadjari, Tchaourom, and Maradouni North show average intensities. Topographically, the

northern and north-western regions correspond to the highest altitudes (275-285 m), whereas the lower zones (285–304 m), including Marafadjari, Tchaourom, Maradouni Nord, Bol, Tandal, Berim 1, Berim 2, and Bol Berim, are characterised by increased vulnerability to flooding (**Figure 5**; **Table 7**). Over 43.27% of the study area, notably Marafadjari, Tchaourom, Maradouni Nord, Bol, Tandal, Berim 1, Berim 2, and Bol Berim, has slopes between 1 and 3%, which correspond to the highest flood-sensitivity scores (**Figure 6**; **Table 7**). Land occupation and use also influence flood risk: built-up areas, accounting for 18.02% of the land and mainly located in Matafo 1, Maradouni Nord, Bol, and Berim, exhibit a high flood score due to their low infiltration capacity. Conversely, vegetation zones (6.72%), crops (6.79%), and open water (14.50%) promote infiltration and runoff (**Figure 7**; **Table 7**). Proximity to the river network further amplifies risk. Areas less than 200 m and between 200 and 500 m from watercourses, covering 13.30% and 20.31% of the area, respectively, are located in the sectors of Bol, Tandal, Berim 1, Berim 2, and Bol Berim, where flooding susceptibility is greatest (**Figure 8**; **Table 7**). Sandy soils, which predominate at 52.95%, facilitate relatively effective infiltration, while clay soils (15.91%) and alluvial or hydromorphic soils (0.38%), predominantly found in Maradouni Nord, Bol, and Berim, tend to have low permeability, contributing to the high flood risk scores observed in these zones (**Figure 9**; **Table 7**). Drainage density in the study area is generally low: classes of 1–4 m/m^2 and 4–10 m/m^2 cover 59.81% and 21.02% of the surface area, respectively, and are associated with low risk. Conversely, the smaller zones with densities between 10 and 34 m/m^2, which constitute 19.17% of the area, are associated with higher risk levels (**Figure 10**; **Table 7**). Lastly, the flow accumulation analysis shows that 95.96% of the area corresponds with low values (0–101 pixels), located in the north, centre, and west. Higher classes, although sparse (1.54% to 0.46% for intermediate and 1.31% to 0.73% for the highest values), are mainly situated along drainage channels crossing Tandal, Bol Berim, Berim 1, and Berim 2, where runoff concentrates, increasing flood risk (**Figure 11**; **Table 7**).

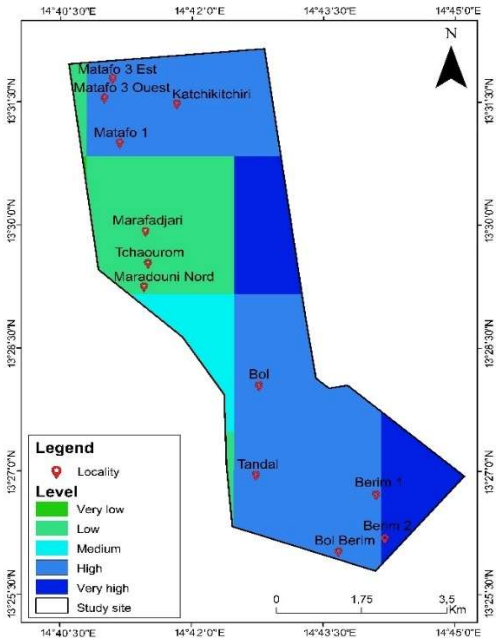

Figure 4. Rainfall intensity.

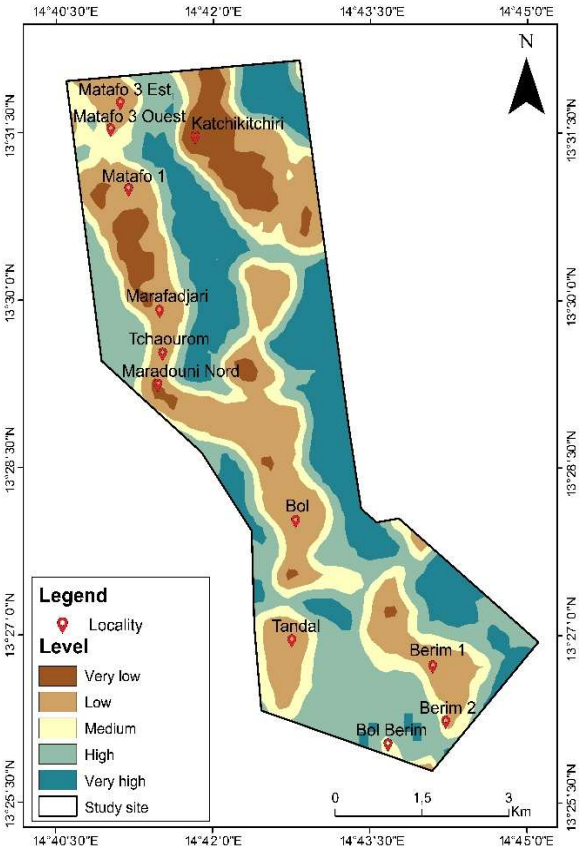

Figure 5. Altitude.

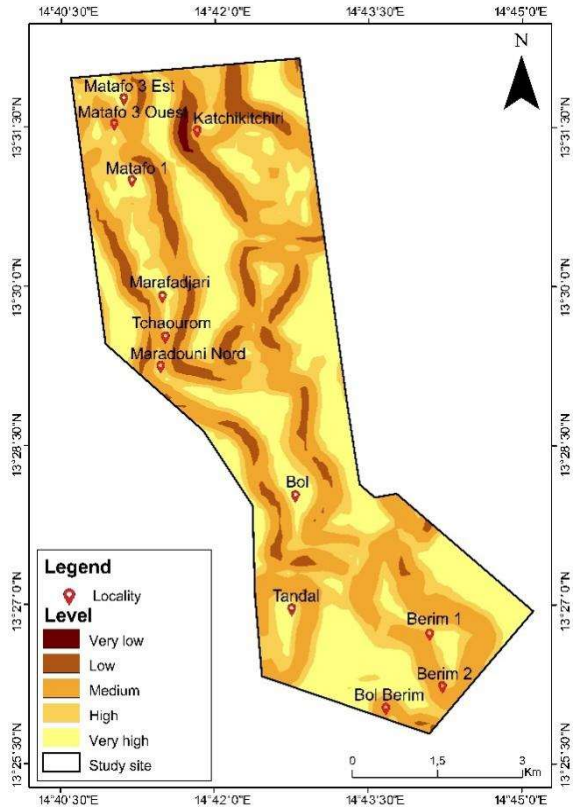

Figure 6. Slope.

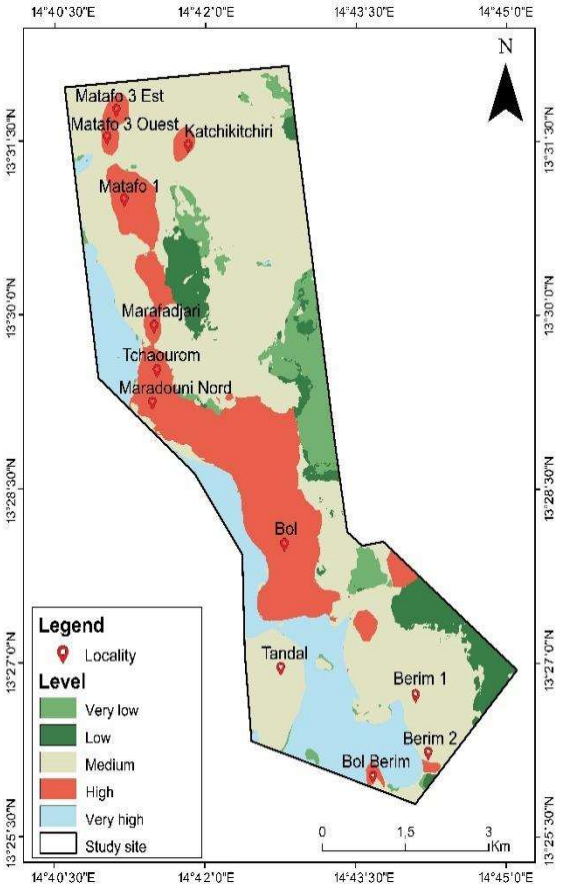

Figure 7. Land use and land cover.

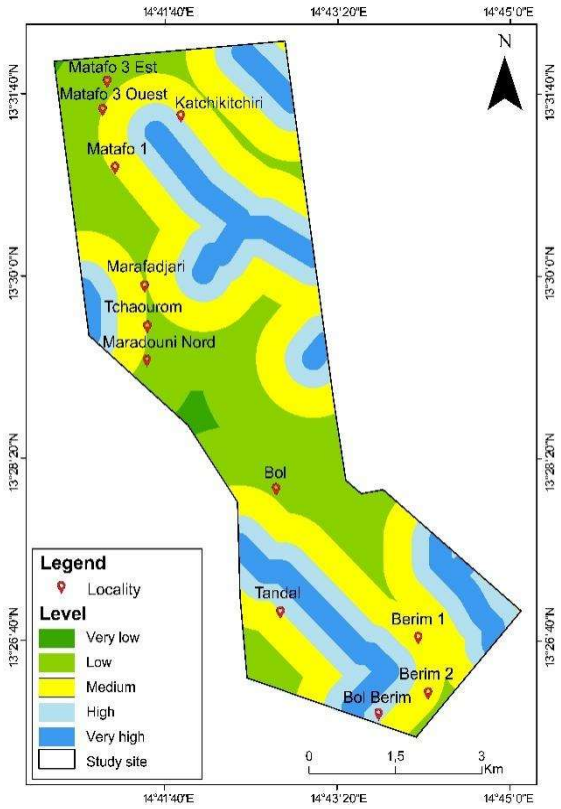

Figure 8. Distance from watercourses.

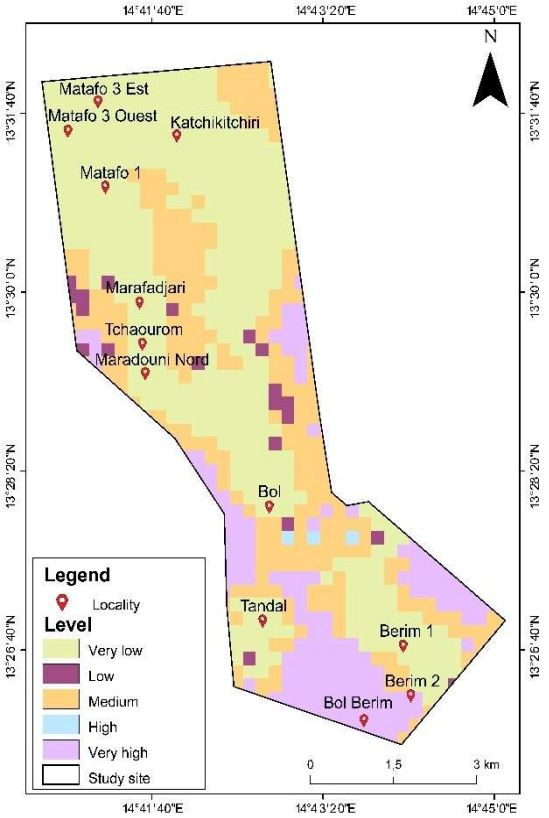

Figure 9. Soil type.

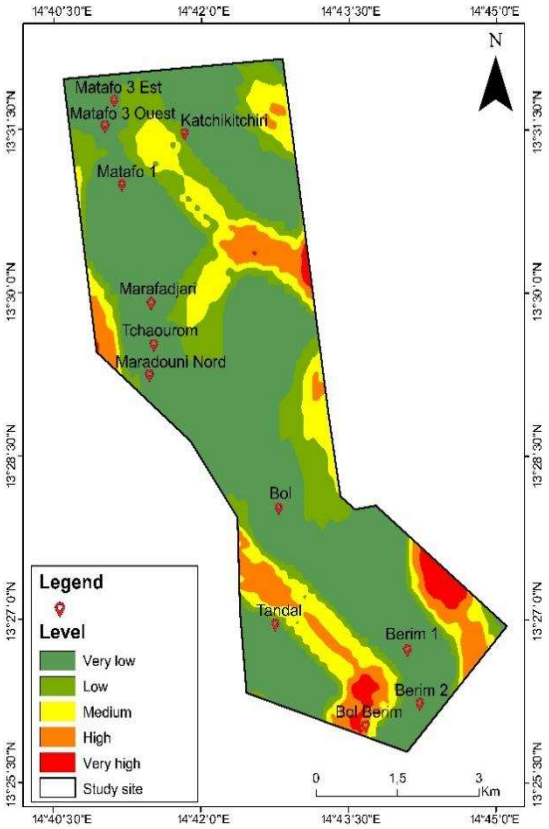

Figure 10. Drainage density.

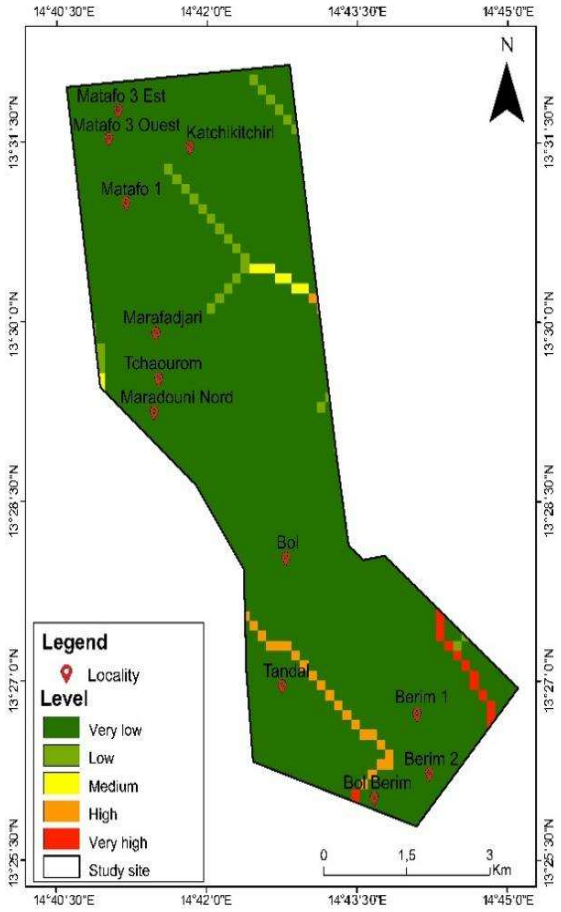

Figure 11. Accumulation of flows.

Beyond surface proportions, the spatial distribution of classes reveals a clear structure of flood susceptibility: low-lying areas with very gentle slopes exhibit the highest levels of risk, as they promote stagnation and runoff accumulation. This pattern is further supported by the presence of hydromorphic or low-permeability soils, which restrict infiltration, and by urbanisation (LULC), which increases runoff. Therefore, regions where low slopes, proximity to the hydrographic network, built-up areas, and low-permeability soils coincide correspond to the main risk zones identified on the thematic maps (**Figures 4–11**), explaining their dominant role in overall susceptibility.

3.2.2. Weighting of factors and flood risk index model

Saaty's AHP model was utilised to estimate the relative importance of factors contributing to the selected floods. The pairwise comparison matrix and the factor weightings are shown in **Table 8**. The AHP hierarchy reveals that factors related to hydrometeorological forcing (precipitation) and topographical context (altitude, slope) are the primary determinants of flood susceptibility. In the case of Bol, this dominance aligns with a flood dynamic driven by the intensity of inflows during the rainy season and the very limited capacity of low-lying areas to drain water. Land use and proximity to the hydrographic network further influence this dynamic by affecting infiltration, runoff, and flow connectivity.

Table 8. Matrice de comparaison par paires et poids estimés.

Factors	Flow accumulation (FA)	Precipitation intensity (PI)	Soil texture (ST)	Land use and land cover (LULC)	Slope (S)	Elevation (E)	Distance from watercourse (DF)	Drainage density (DD)	Weight
Flow accumulation (FA)	1	1/8	1/3	1/4	1/6	1/7	1/4	½	0.03
Precipitation intensity (PI)	8	1	8/3	2	4/3	8/7	2	4	0.23
Soil texture (ST)	3	3/8	1	3/4	1/2	3/7	3/4	3/2	0.09
Land use and land cover (LULC)	4	1/2	4/3	1	2/3	4/7	1	2	0.11
Slope (S)	6	3/4	2	7/4	1	6/7	3/2	3	0.17
Elevation (E)	7	7/8	7/3	7/4	7/6	1	7/4	7/2	0.20
Distance from watercourse (DF)	4	1/2	4/3	1	2/3	4/7	1		0.11
Drainage density (DD)	2	1/4	2/3	1/2	1/3	2/7	1/2	1	0.06
CR=0.0042									

Furthermore, the calculated RC value is 0.0042. Since it remains below the critical threshold of 0.1, the weights determined are deemed consistent and suitable for use in calculating the flood hazard index, as shown in Equation (7).

$$FHI = 0{,}03X_{FA} + 0{,}23X_{PI} + 0{,}09X_{\mathbf{ST}} + 0{,}11X_{\mathbf{LULC}} + 0{,}17X_{\mathbf{S}} + 0{,}20X_{E} + 0{,}11X_{DF} + 0{,}06X_{DD} \quad (7)$$

Based on the factor weightings, rainfall intensity has the highest weight in the city of Bol, indicating that it is the primary factor contributing to the risk of flooding there.

3.2.3. Flood susceptibility map for the city of Bol

The flood susceptibility map (**Figure 12**) was created by combining eight physical factors using coefficients derived from the Analytical Hierarchy Process (AHP). The results (**Figure 12** and **Table 9**) show that 16.19% of the city of Bol is at very high flood risk, while 28.08% is at high risk. These highly vulnerable zones are mainly clustered around Bol, Tandal, Berim 1, Berim 2, and Bol Berim. Conversely, very low and low risk levels cover 11.29% and 17.72% of the total area, primarily in the north and north-west, particularly in Matafo 3 East and West, Marafadjari, Tchaourom, Maradouni North, and Katchikitchiri. The medium risk class, accounting for 26.72% of Bol, encompasses intermediate zones situated between these extremes, notably around Marafadjari, Tchaourom, and Maradouni North. Additionally, the results indicate that high- and very high-risk zones correspond to areas with the highest rainfall intensities, confirming that rainfall intensity is the primary factor influencing physical vulnerability to flooding in Bol. Finally, the spatial analysis (**Figure 12**) reveals an uneven distribution of risk, reflecting significant spatial heterogeneity associated with the eight physical factors considered in this analysis.

Table 9. Area distribution of hazard levels.

Danger level	Surface area	Percentage (%)
Very low	469.28	11.29
Low	736.95	17.72
Medium	1111.06	26.72
High	1167.83	28.08
Very high	673.43	16.19
TOTAL	4158.55	100

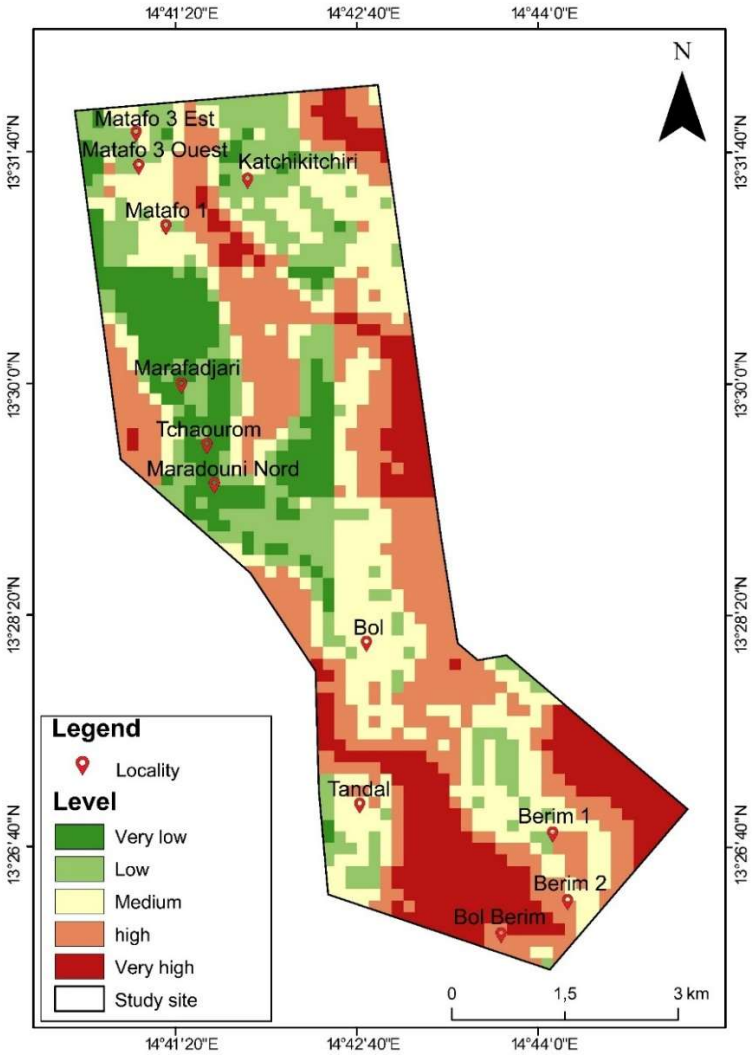

Figure 12. Flood susceptibility map of the city of Bol using the AHP model.

Figure 12 shows that moderate-to-high susceptibility classes are mainly concentrated in low-lying areas with gentle slopes, where hydrological connectivity is enhanced by the proximity of the drainage network. Areas with low susceptibility are more likely to be relatively higher and better drained. This spatial organisation is consistent with the maps of dominant factors (**Figures 4–11**), suggesting that susceptibility results from the combination of unfavourable topographical conditions and surface characteristics that limit infiltration.

3.3. Relationship between the flood susceptibility map, data from field surveys conducted in 2024, and the built-up area of the city of Bol

3.3.1. Relationship between the flood susceptibility map and the built-up area of the city of Bol in 2024

Of the city of Bol's total area of 4,158.55 ha, built-up areas occupy 749.30 ha, or 18.02% of the total urban area. The superimposition of the flood susceptibility map, developed from remote sensing data and the combined GIS-AHP approach, with land use is shown in **Figure 13**, where built-up areas appear in pink. The results (**Figure 13** and **Table 10**) indicate that 41.95% (314.37 ha) of the built-up area is in areas classified as having a very low to low flood risk (15.11% very low and 26.84% low), which reflects a relatively limited exposure to flooding. On the other hand, 47.12% (353.07 ha) of the built-up area is in areas of moderate sensitivity, while 10.93% (81.86 ha) is in areas characterised by high to very high risk (including 10.57% at high risk and 0.36% at very high risk). As illustrated in **Figure 13**, a significant proportion of the built-up area is in moderate to high susceptibility classes, indicating potential exposure of the habitat to flooding and justifying the use of urban-scale mapping to guide zoning and risk reduction measures.

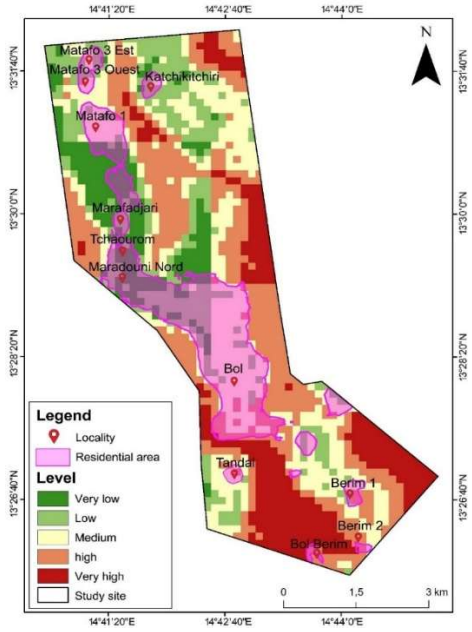

Figure 13. Comparison of the flood susceptibility map with the extent of built-up areas in 2024.

Table 10. Distribution of built-up area according to hazard level.

Danger level	Built-up area (ha)	Percentage (%)
Very low	113.22	15.11
Low	201.15	26.84
Medium	353.07	47.12
High	79.19	10.57
Very high	2.67	0.36
TOTAL	749.30	100

3.3.2. Relationship between the flood susceptibility map and household surveys conducted in Bol in 2024

The results of the comparison between the flood susceptibility map developed using GIS and the AHP method (**Figure 14**) and the field survey data collected in 2024 are presented in **Figure 14** and **Table 11**. The 385 households surveyed are georeferenced and represented as points on the map (**Figure 14**). The results indicate that 38.96% of households are in areas characterised by very low to low risk (9.35% and 29.61%, respectively), while 39.74% are in areas of moderate risk. Furthermore, 21.30% of households are in high-risk areas, while no households are recorded in areas classified as very high risk. A χ^2 goodness-of-fit test applied to the distribution of households surveyed according to flood susceptibility classes reveals a highly significant difference from a uniform distribution ($\chi^2 = 191.95$; $ddl = 4$; $p < 0.001$), indicating a marked concentration of households in areas of moderate to high susceptibility.

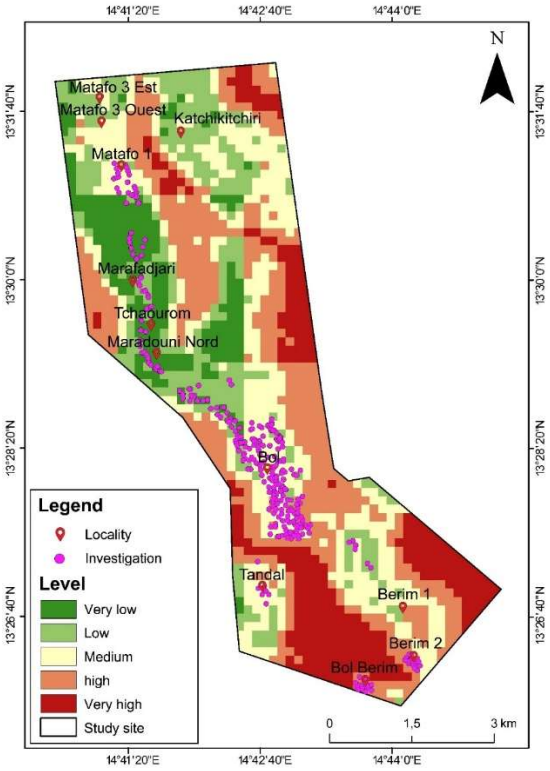

Figure 14. Comparison of the flood susceptibility map with the 2024 household surveys.

Table 11. Distribution of households according to level of risk.

Danger level	Number of households	Percentage (%)
Very low	36	09,35
Low	114	29,61
Medium	153	39,74
High	82	21,30
Very high	00	00
Total	385	100

4. Discussion

The results of this research show that the households surveyed in Bol are characterised by a strong male predominance (87.01%) and a population mainly of working age (20–59 years: 85.46%), which is common in surveys conducted in Sahelian cities, where heads of households and main respondents are predominantly men, due to socio-cultural norms and gendered division of roles [59]. This configuration influences risk perception and adaptation choices, which are often made by household heads rather than by all household members, particularly women and the elderly. Furthermore, analysis of place of birth reveals that more than 84% of respondents are natives of Bol or the Lake Province, indicating a largely indigenous, permanently settled population. This long-term residence may reinforce empirical knowledge of risks, particularly flooding, as shown by several studies in sub-Saharan Africa, where local populations develop adaptation strategies based on accumulated experience [60,61]. However, this familiarity with hazards can also promote a normalisation of risk, as illustrated by the fact that nearly half of those surveyed (49.87%) perceive flooding as an annual phenomenon. This process has already been documented in the literature on climate risk perception by Doussoumou et al. [62] and Kumaresen et al. [63], who show that the near-annual recurrence of floods tends to render them "ordinary" hazards. Furthermore, the majority perception of regular (70.91%) and intense (58.70%) rainfall is consistent with several studies conducted in sub-Saharan Africa, which highlight an increase in the intensity of extreme rainfall rather than a uniform increase in annual rainfall, thereby increasing the risk of urban flooding [64,65]. This rainfall pattern promotes high runoff volumes over short periods, quickly exceeding the soil's and urban drainage systems' absorption and drainage capacities, thereby increasing susceptibility to flooding. These perceptions and physical conditions are reflected in the high proportion of households reporting that they were affected by the 2024 floods (63.90%) and suffered loss of housing (38.70%), which is consistent with the studies by Allarané et al. [28] on the direct impacts of flooding in N'Djamena, where material damage is one of the most frequent and severe consequences.

In spatial terms, the flood susceptibility mapping carried out in Bol highlights the central role of the combination of physical flood factors, namely rainfall intensity, altitude, slope, land use and cover, distance to watercourses, soil infiltration capacity, drainage network density, and flow accumulation in a GIS environment. The high weighting given to rainfall intensity in the AHP analysis confirms its decisive role, as shown in numerous previous studies [24,36,41]. However, the literature emphasises that the dominant factor varies according to the hydro-geomorphological and urban context: some studies give greater weight to distance from watercourses [7,38], soil properties [45], altitude [23], slope [38,43], land use and cover [40], flow accumulation [27] or drainage network density [38]. The case of Bol is distinguished by its location in a low-relief lake plain, where slight variations in altitude are sufficient to promote water accumulation and stagnation.

The results of this study show that 44.27% of the city of Bol is exposed to a high to very high risk of flooding (28.08% and 16.19%, respectively). These areas mainly correspond to agricultural polders and areas adjacent to watercourses. This high

vulnerability can be explained by a combination of intense rainfall, gentle slopes, low altitudes, proximity to watercourses and the presence of clay soils, which promote water accumulation and stagnation. These results are consistent with the conclusions of [66,67]. They also agree with those of Quesada-Román [68] in Costa Rica, who emphasise that the highest flood risks are concentrated in areas with low slopes, low altitudes and clay soils. Furthermore, 26.72% of the city of Bol's area has a medium level of risk, indicating significant vulnerability to flooding. In contrast, low- and very low-risk areas cover only 29.01% of the total area (17.72% and 11.29% respectively). These areas are mainly located in the north and north-west, where higher altitudes, greater distance from watercourses, better soil permeability, better drainage and relatively low rainfall contribute to reducing the risk of flooding. These conclusions are consistent with those of [7,69], which emphasised that topographical, pedological and other environmental factors play an important role in reducing flood risks.

The relative contribution of these factors was quantified using a multi-criteria decision-making approach based on the analytical hierarchy process (AHP) developed by Thomas Saaty [54], which relies on pairwise comparisons and the estimation of normalised weights reflecting the relative importance of each parameter. The analytical hierarchy process (AHP) is a structured decision-making framework that helps prioritise and select the best option by breaking a complex decision into a hierarchy of objectives, criteria, and alternatives [26]. It improves decision-making by providing clearer visualisation and enhanced mapping capabilities, thereby facilitating the development of hazard maps [18]. Nevertheless, AHP is subject to several methodological criticisms, particularly its unbalanced judgment levels, arbitrary rankings, high subjectivity in scoring, and inability to accurately handle the uncertainty associated with pairwise comparisons [70,71]. Furthermore, psychological research has shown that nine items represent the maximum number a person can reliably rank and compare simultaneously; hence, it is strongly recommended to use no more than nine criteria [7,72], which highlights the limitation of this study to eight (8) factors. Despite these limitations, AHP remains an effective and relevant method for risk mapping [53,73], as it allows complex decisions to be structured and expert knowledge to be integrated in contexts where data are limited, while ensuring rigorous control over the consistency of judgments.

An important methodological contribution of this study lies in the validation of results by field data. The statistically significant concentration of affected households in the moderate-to-high susceptibility classes, as highlighted by the χ^2 test, reinforces the credibility of the GIS-AHP model. Few GIS-AHP studies include explicit socio-spatial validation, often limiting themselves to a visual comparison of maps and observations [27,57]. In this respect, the approach adopted is in line with the recommendations of ref. [74], which calls for better coordination between spatial modelling and social data to improve the operational relevance of vulnerability maps.

However, this study's methodological limitations must be discussed. The subjectivity inherent in AHP, linked to expert judgements and weighting choices, has been highlighted by Malczewski [75], who warns against the sensitivity of results to methodological decisions. Feizizadeh et al. [76] therefore recommend using sensitivity analyses or variants, such as fuzzy AHP, to better integrate the uncertainty associated with pairwise comparisons. The use of moderate-resolution global data is a common

compromise in regions with low local data production capacities. However, as Merz et al. [77] point out, this choice may limit accuracy at the intra-urban scale and warrants caution in the detailed interpretation of results, particularly in transition zones between susceptibility classes. Furthermore, harmonising data from global sources and heterogeneous spatial resolutions can introduce smoothing effects, potentially affecting local spatial accuracy, particularly in transition zones between susceptibility classes. The absence of formal uncertainty and sensitivity analysis is therefore a significant limitation of this study.

Despite these limitations, the susceptibility map produced is a relevant operational tool for flood risk management in Bol. It identifies priority areas for urban development, drainage infrastructure planning and housing adaptation. It can be used not only to raise awareness among communities, construction stakeholders, and decision-makers about the most exposed areas, but also to help them implement measures to strengthen their resilience, such as construction techniques, material choices, and construction types specific to each area. In addition, the flood risk susceptibility map plays a key role in land use and urban planning by providing information to define the functions, priorities, and constraints specific to each area of the city. This approach is important because over the last two decades, the frequency of flooding has increased, not only due to climate variability but also to anthropogenic factors such as rapid and unplanned urbanisation, deforestation, increased extraction of aggregates for construction, inappropriate agricultural practices, and poor soil and waste management [7,65,78,79]. This approach provides a solid scientific basis for supporting decision-making and strengthening urban resilience.

5. Conclusions

This study aims to characterise the physical susceptibility to flooding in the city of Bol in order to contribute to better management of a risk that has become increasingly recurrent in this Sahelian urban context. It also assessed the combined contribution of remote sensing, geographic information systems (GIS) and the Analytic Hierarchy Process (AHP) to identifying and prioritising areas vulnerable to flooding.

Methodologically, the study used eight key physical factors: rainfall intensity, altitude, slope, land use and cover, distance to watercourses, soil infiltration capacity, drainage network density and flow accumulation, integrated into a GIS environment. Weighting these factors using AHP produced a susceptibility map showing that 44.27% of Bol's urban area is highly to very highly susceptible to flooding, reflecting significant structural exposure linked to local hydro-geomorphological conditions and unplanned occupation of low-lying areas. Field surveys also revealed a predominantly male, active, and indigenous population, characterised by a high dependence on economic activities sensitive to climate hazards, as well as a marked perception of intense rainfall and recurrent flooding, as confirmed by the significant impacts of the 2024 events.

The results obtained highlight the value of the GIS-AHP approach as a decision-making tool for urban planning, drainage infrastructure design and prioritisation of areas for flood risk reduction interventions. As such, the susceptibility map produced

is a relevant operational tool for local decision-makers, urban planners, architects and disaster management services.

However, the scope of this study must be interpreted in light of several limitations. On the one hand, the analysis focuses exclusively on physical vulnerability (susceptibility) and omits the dimensions of exposure and adaptive capacity, which are essential to a comprehensive assessment of flood risk. Secondly, the use of global datasets, due to the limited availability of high-resolution local data, may affect the spatial accuracy of the results, particularly at the intra-urban scale. Finally, the lack of in-depth quantitative validation and formal analysis of uncertainties in factor weighting is a significant methodological limitation.

Future research should therefore focus on an integrated assessment of flood risk, combining susceptibility, exposure and adaptive capacity, while utilising higher-resolution local data and quantitative validation and sensitivity analysis methods. Exploring complementary approaches, such as fuzzy AHP or hybrid methods, would also allow for better consideration of the uncertainties associated with expert judgements.

Despite these limitations, this study makes a significant scientific and operational contribution to understanding flood vulnerability in the city of Bol and more broadly in Sahelian cities. It provides a solid basis for integrating flood risk management into urban development policies and local climate change adaptation strategies in the Lac province of Chad.

Author contributions: Conceptualization, PAT ; methodology, PAT, FTN, KK and AKD; software, PAT, FTN, AR and PB; validation, AKB, KK and AR; formal analysis, PAT and AR; investigation, PAT, PB and AR; resources, PAT and KSK. data curation, PAT and AR; writing—original draft preparation, PAT; writing—review and editing, PAT, FTN, KK and AKD; visualization, KSK, KK, and AKD; supervision, KSK; project administration, KSK; funding acquisition, PAT. All authors have read and agreed to the published version of the manuscript.

Funding: The World Bank supported this work through the Regional Centre of Excellence on Sustainable Cities in Africa (CERViDA-DOUNEDON). The funding numbers are 6512-TG and 5360-TG.

Ethical approval: Ethical approval was obtained from the Regional Ethics Committee of CERVIDA-DOUNEDON at the thesis stage of the 2022-2023 academic year (266/D/CERViDA-DOUNEDON/UL/2022). All participants provided informed written consent before their involvement in the research.

Acknowledgments: The authors thank the Regional Centre of Excellence on Sustainable Cities in Africa (CERViDA-DOUNEDON), the Association of African Universities, and the World Bank Group for their financial support.

Conflict of interest: The authors declare no conflict of interest.

References

1. Deng M, Qin D, Zhang H. Public perceptions of climate and cryosphere change in typical arid inland river areas of China: Facts, impacts and selections of adaptation measures. Quaternary International. 2012; 282: 48–57. doi: 10.1016/j.quaint.2012.04.033

2. Ahmad B, Nadeem M, Hussain S, et al. People's perception of climate change impacts on subtropical climatic region: A case study of upper indus, Pakistan. Climate. 2024; 12(5): 73. doi: 10.3390/cli12050073
3. Onus EL, Chinyio E, Daniel EI. 'Stakeholder Perceptions' of the impacts of climatic features on residents and residences: A UK study. Atmosphere. 2024; 15(7): 791. doi: 10.3390/atmos15070791
4. Majlingova A, Kádár TS. From Risk to Resilience: Integrating Climate Adaptation and Disaster Reduction in the Pursuit of Sustainable Development. Sustainability. 2025; 17(12): 5447. doi: 10.3390/su17125447
5. IPCC GIEC, GTII, Sixième Évaluation, Chapitre 6. 2022, Climate Change 2022: Impacts, Adaptation and Vulnerability|Climate Change 2022: Impacts, Adaptation and Vulnerability. Available online: https://www.ipcc.ch/report/ar6/wg2/ (accessed on 26 August 2025).
6. Nguyen DN, Usuda Y, Imamura F. Gaps in and opportunities for disaster risk reduction in Urban Areas through international standardization of smart community infrastructure. Sustainability. 2024; 16(21): 9586. doi: 10.3390/su16219586
7. Blakime TH, Komi K, Adjonou K, et al. Derivation of a GIS-Based flood hazard map in Peri-Urban areas of greater Lomé, Togo (West Africa). Urban Science. 2024; 8(3): 96. doi: 10.3390/urbansci8030096
8. Ibeanu C, Ghadiri Nejad M, Ghasemi M. Developing effective project management strategy for urban flood disaster prevention project in edo state capital, nigeria. Urban Science. 2023; 7(2): 37. doi: 10.3390/urbansci7020037
9. Scolozzi R, Scolobig A, Borga M. Public support for flood risk management: insights from an Italian alpine survey using systems thinking. Geographies. 2025; 5(1): 3. doi: 10.3390/geographies5010003
10. World Health Organization Floods. Available online: https://www.who.int/health-topics/floods#tab=tab_1 (accessed on 19 December 2025).
11. Floods in the Sahel: Nearly 600 dead and people still waiting for government promises of resilient infrastructure (French). Available online: https://www.bbc.com/afrique/articles/cwy30825gxgo (accessed on 3 June 2025).
12. Djako EG, Mendy E, Ngaryamgaye S, et al. Study of the gendered impacts of climate change in Bol, Lake Province, Chad. Climate. 2024; 12(10): 157. doi: 10.3390/cli12100157
13. In Chad, the president declares a state of emergency in response to flooding (French). Available online: https://www.france24.com/fr/afrique/20221020-au-tchad-le-pr%C3%A9sident-d%C3%A9cr%C3%A8te-un-%C3%A9tat-d-urgence-face-aux-inondations (accessed on 2 June 2025).
14. Adoum AA. Organic matter and carbon storage in the soils of polders in the north-eastern Bol region of Lake Chad in the context of global changes in semi-arid environments (French). L'Institut des Sciences et Industries du Vivant et de l'Environnement (AgroParisTech): Paris; 2016.
15. Djako EG, Allarané N, Aigbavboa C, et al. Evaluation of urban planning practices in Bol city, Lake Province (Chad): Challenges and prospects. Journal of Infrastructure Policy and Development. 2025; 9(2): 11111. doi: 10.24294/jipd11111
16. D Djako EG, Aboukey G, Azianu KA, et al. Spatiotemporal dynamics and humanitarian crisis in Bol (Chad): Satellite imagery analysis. Edelweiss Applied Science and Technology. 2025; 9(5): 2923–2939. doi: 10.55214/25768484.v9i5.7617
17. Amigué SP. Lake Chad: The sons of the lake united in the face of flooding (French). Available online: https://www.alwihdainfo.com/Lac-Tchad-Les-fils-du-Lac-unis-face-aux-inondations_a135566.html (accessed on 3 June 2025).
18. Sajid T, Maimoon SK, Waseem M, et al. Integrated risk assessment of floods and landslides in kohistan, pakistan. Sustainability. 2025; 17(8): 3331. doi: 10.3390/su17083331
19. Baghermanesh SS, Jabari S, McGrath H. Urban flood detection using terra SAR-X and SAR simulated reflectivity maps. Remote Sensing. 2022; 14(23): 6154. doi: 10.3390/rs14236154
20. Sajjad A, Lu J, Chen X, et al. Rapid assessment of riverine flood inundation in Chenab floodplain using remote sensing techniques. Geoenvironmental Disasters. 2023; 10(1): 9. doi: 10.1186/s40677-023-00236-7
21. Marti-Cardona B, Lopez-Martinez C, Dolz-Ripolles J, et al. ASAR polarimetric, multi-incidence angle and multitemporal characterization of Doñana wetlands for flood extent monitoring. Remote Sensing of Environment. 2010; 114(11): 2802–2815. doi: 10.1016/j.rse.2010.06.015
22. Huang M, Jin S. Rapid Flood Mapping and evaluation with a supervised classifier and change detection in Shouguang Using Sentinel-1 SAR and Sentinel-2 optical data. Remote Sensing. 2020; 12(13): 2073. doi: 10.3390/rs12132073
23. Alarifi SS; Abdelkareem M, Abdalla F; et al. Flash flood hazard mapping using remote sensing and DIS techniques in southwestern Saudi Arabia. Sustainability. 2022; 14: 14145. doi: 10.3390/su142114145
24. Allafta, H; Opp, C. GIS-Based multi-criteria analysis for flood prone areas mapping in the trans-boundary shatt al-arab basin, Iraq-Iran. Geomatics, Natural Hazards and Risk. 2021; 12: 2087–2116. doi: 10.1080/19475705.2021.1955755.

25. Morea, H, Samanta, S. Multi-Criteria decision approach to identify flood vulnerability zones using geospatial technology in the kemp-welch catchment, central province, Papua new guinea. Appl Geomat 2020, 12, 427–440, doi:10.1007/s12518-020-00315-6.
26. Mokhtari E, Mezali F, Abdelkebir B, et al. Flood risk assessment using analytical hierarchy process: A case study from the Cheliff-Ghrib watershed, Algeria. Journal of Water and Climate Change. 2023; 14(3): 694–711. doi: 10.2166/wcc.2023.316
27. Kazakis N, Kougias I, Patsialis T. Assessment of Flood Hazard Areas at a Regional Scale Using an Index-Based Approach and Analytical Hierarchy Process: Application in Rhodope–Evros Region, Greece. Science of The Total Environment. 2015; 538: 555–563. doi: 10.1016/j.scitotenv.2015.08.055
28. Allarané N, Azagoun VVA, Atchadé AJ, et al. Urban vulnerability and adaptation strategies against recurrent climate risks in Central Africa: Evidence from N'Djaména City (Chad). Urban Science. 2023; 7: 97. doi: 10.3390/urbansci7030097
29. Abdelkerim KW, Bogaide ZE. Inondation en milieu Urbain, cas du 9ème arrondissement de la ville de N'Djaména (Cité-Capitale du Tchad). 36. https://edition-efua.acaref.net/wp-content/uploads/sites/6/2025/02/1-ABDELKERIM-Korme-Wachi.pdf.
30. Djimta R, Fourissou M, Pamdegue F, et al. « Flood risk management in the city of N'Djamena, Chad (French), contributions of remote sensing and geographic information systems». Annales de l'Université de N'Djaména 2024; 20.
31. Gbetkom PG, Crétaux JF, Tchilibou M, et al. Lake Chad vegetation cover and surface water variations in response to rainfall fluctuations under recent climate conditions (2000−2020). Science of The Total Environment. 2023; 857: 159302. doi: 10.1016/j.scitotenv.2022.159302
32. Sylvestre F, Mahamat-Nour A, Naradoum T, et al. Strengthening of the hydrological cycle in the Lake Chad Basin under current climate change. Scientific Reports. 2024; 14(1): 24639. doi: 10.1038/s41598-024-75707-4
33. Okeke-Ogbuafor N, Gray T, Ani K, et al. Proposed solutions to the problems of the lake chad fisheries: Resilience lessons for Africa? Fishes. 2023; 8(2): 64. doi: 10.3390/fishes8020064
34. Olowoyeye OS, Kanwar RS. Water and food sustainability in the riparian countries of lake chad in africa. Sustainability. 2023; 15(13): 10009. doi: 10.3390/su15131000
35. Negese A, Worku D, Shitaye A, et al. Potential flood-prone area identification and mapping using GIS-based multi-criteria decision-making and analytical hierarchy process in Dega Damot district, northwestern Ethiopia. Applied Water Science. 2022; 12(12): 255. doi: 10.1007/s13201-022-01772-7
36. Taoukidou N, Karpouzos D, Georgiou P. Flood hazard assessment through AHP, fuzzy AHP, and frequency ratio methods: A comparative analysis. Water. 2025; 17(14): 2155. doi: 10.3390/w17142155
37. Koroma AO, Saber M, Abdelbaki C. Urban flood vulnerability assessment in Freetown, Sierra Leone: AHP Approach. Hydrology. 2024; 11(10): 158. doi: 10.3390/hydrology11100158
38. Oyedele P, Kola E, Olorunfemi F, et al. Understanding flood vulnerability in local communities of Kogi state, Nigeria, using an index-based approach. Water. 2022; 14: 2746. doi: 10.3390/w14172746
39. Sarker S, Jahan I, Wang X, et al. Geospatial approach to assess flash flood vulnerability in a coastal district of bangladesh: integrating the multifaceted dimension of vulnerabilities. ISPRS International Journal of Geo-Information. 2025; 14(5): 194. doi: 10.3390/ijgi14050194
40. Aichi A, Ikirri M, Ait Haddou M, et al. Integrated GIS and analytic hierarchy process for flood risk assessment in the dades wadi watershed (central high atlas, morocco). Results in Earth Sciences. 2024; 2: 100019. doi: 10.1016/j.rines.2024.100019
41. Ikirri M, Faik F, Echogdali FZ, et al. Flood hazard index application in arid catchments: case of the taguenit wadi watershed, lakhssas, morocco. Land. 2022; 11(8): 1178. doi: 10.3390/land11081178
42. Shrestha S, Dahal D, Poudel B, et al. Flood susceptibility analysis with integrated geographic information system and analytical hierarchy process: A multi-criteria framework for risk assessment and mitigation. Water. 2025; 17(7): 937. doi: 10.3390/w17070937
43. Tarhule A. Damaging rainfall and flooding: the other sahel hazards. Climatic Change. 2005; 72(3): 355–377. doi: 10.1007/s10584-005-6792-4
44. Mojaddadi H, Pradhan B, Nampak H, et al. Ensemble machine-learning-based geospatial approach for flood risk assessment using multi-sensor remote-sensing data and GIS. Geomatics, Natural Hazards and Risk. 2017; 8(2): 1080–1102. doi: 10.1080/19475705.2017.1294113
45. Barboza TOC, Ferraz MAJ, Pilon C, et al. Advanced farming strategies using NASA POWER data in peanut-producing regions without surface meteorological stations. AgriEngineering. 2024; 6(1): 438–454. doi: 10.3390/agriengineering6010027

46. Tóth B, Weynants M, Pásztor L, et al. 3D soil hydraulic database of Europe at 250 m resolution. Hydrological Processes. 2017; 31(14): 2662–2666. doi: 10.1002/hyp.11203
47. Mahmoud SH, Gan TY. Multi-criteria approach to develop flood susceptibility maps in arid regions of middle east. Journal of Cleaner Production. 2018; 196: 216–229. doi: 10.1016/j.jclepro.2018.06.047
48. Mahmoud, SH; Gan, TY. Multi-Criteria approach to develop flood susceptibility maps in arid regions of middle east. Journal of Cleaner Production 2018; 196: 216–229, doi: 10.1016/j.jclepro.2018.06.047.
49. Komi, K. Physical flood vulnerability mapping using the analytical hierarchy process method and geography information system: application to the savannah region, TOGO (West Africa), International Roundtable on the Impact of Extreme Natural Events: Science and Technology for Mitigation; 2017.
50. Senanou G, Ayarema A, Samah ODE, et al. Projection on intensity duration frequency curves in a context of climate change in the city of Lomé (West Africa). IJAR. 2019; 7: 678–692. doi: 10.21474/IJAR01/9271
51. Chowdhuri I, Pal SC, Chakrabortty R. Flood susceptibility mapping by ensemble evidential belief function and binomial logistic regression model on river basin of Eastern India. Advances in Space Research. 2020; 65: 1466–1489. doi: 10.1016/j.asr.2019.12.003
52. Rimba AB, Chapagain SK, Masago Y, et al. Investigating water sustainability and land use/land cover change (LULC) as the impact of tourism activity in bali, indonesia. IGARSS 2019 - 2019 IEEE international geoscience and remote sensing symposium. IEEE. 2019: 6531–6534. doi: 10.1109/igarss.2019.8900060
53. Canco I, Kruja D, Iancu T. AHP, a reliable method for quality decision making: A case study in business. Sustainability. 2021; 13(24): 13932. doi: 10.3390/su132413932
54. Saaty TL, Vargas LG. Inconsistency and rank preservation. Journal of Mathematical Psychology. 1984; 28: 205–214. doi: 10.1016/0022-2496(84)90027-0
55. Bozóki S, Fülöp J. Efficient weight vectors from pairwise comparison matrices. European Journal of Operational Research. 2018; 264(2): 419–427. doi: 10.1016/j.ejor.2017.06.033
56. Wu J, Chen X, Lu J. Assessment of long and short-term flood risk using the multi-criteria analysis model with the AHP-Entropy method in Poyang Lake basin. International Journal of Disaster Risk Reduction. 2022; 75: 102968. doi: 10.1016/j.ijdrr.2022.102968
57. Rahmati O, Zeinivand H, Besharat M. Flood hazard zoning in Yasooj region, Iran, using GIS and multi-criteria decision analysis. Geomatics, Natural Hazards and Risk. 2015; 7(3): 1000–1017. doi: 10.1080/19475705.2015.1045043
58. Tombar PA. Abdou KD, Vidjinnagni VAA, et al. Spatial organisation of housing and factors influencing residential choice in the town of bol, lake province, chad. Journal of Building Material Science. 2025; 7(2): 58–79. doi: 10.30564/jbms.v7i2.9374
59. UN-Habitat: Nairobi. The State of African Cities 2014: Re-Imagining Sustainable Urban Transitions. The State of African Cities. UN-Habitat: Nairobi; 2014.
60. Adger WN, Barnett J, Brown K, et al. Cultural dimensions of climate change impacts and adaptation. Nature Climate Change. 2012; 3(2): 112–117. doi: 10.1038/nclimate1666
61. Satterthwaite D, Archer D, Colenbrander S, et al. Building resilience to climate change in informal settlements. One Earth. 2020; 2(2): 143–156. doi: 10.1016/j.oneear.2020.02.002
62. Dossoumou NIP, Gnazou MDT, Villamor GB, et al. Comparing households' perception of flood hazard with historical climate and hydrological data in the lower mono river catchment (West Africa), Benin and Togo. PLOS Clim. 2023; 2: e0000123. doi: 10.1371/journal.pclm.0000123
63. Kumaresen M, Teo FY, Selvarajoo A, et al. Assessing community perception, preparedness, and adaptation to urban flood risks in Malaysia. Water. 2025; 17(15): 2323. doi: 10.3390/w17152323
64. Gbobaniyi E, Sarr A, Sylla MB, et al. Climatology, annual cycle and interannual variability of precipitation and temperature in CORDEX simulations over West Africa. International Journal of Climatology. 2013; 34(7): 2241–2257. doi: 10.1002/joc.3834
65. Klassou KS. Human influence on the origin and severity of flooding in Togo: The case of land use planning in the northern suburbs of Lomé (Togblé-Adétikopé) (French). Revue de Géographie Tropicale et d'Environnement; 2014.
66. Mishra, K; Sinha, R. Flood Risk Assessment in the Kosi Megafan using multi-criteria decision analysis: A Hydro-Geomorphic Approach. Geomorphology. 2020; 350: 106861. doi: 10.1016/j.geomorph.2019.106861.
67. Lyu HM, Sun WJ, Shen SL, et al. Flood risk assessment in metro systems of mega-cities using a GIS-based modeling approach. Science of The Total Environment. 2018; 626: 1012-1025. doi: 10.1016/j.scitotenv.2018.01.138

68. Quesada-Román A. Flood risk index development at the municipal level in Costa Rica: A methodological framework. Environmental Science & Policy. 2022; 133: 98–106. doi: 10.1016/j.envsci.2022.03.012
69. Al-Rawas G, Nikoo MR, Al-Wardy M. A review on the prevention and control of flash flood hazards on a global scale: Early warning systems, vulnerability assessment, environmental, and public health burden. International Journal of Disaster Risk Reduction. 2024; 115: 105024. doi: 10.1016/j.ijdrr.2024.105024
70. Bafahm A, Sun M. Some conflicting results in the analytic hierarchy process. International Journal of Information Technology & Decision Making. 2019; 18(02): 465–486. doi: 10.1142/s0219622018500517
71. Munier, N.; Hontoria, E. Shortcomings of the AHP Method. In uses and limitations of the AHP method; Management for professionals; Springer International Publishing: Cham; 2021. pp. 41–90.
72. Shuaibu A, Hounkpè J, Bossa YA, et al. Flood risk assessment and mapping in the Hadejia River Basin, Nigeria, Using Hydro-Geomorphic approach and multi-criterion decision-making method. Water. 2022; 14(22): 3709. doi: 10.3390/w14223709
73. Makkulawu AR, Soemarno, Santoso I, et al. Exploring the potential and benefits of AHP and GIS integration for informed decision-making: A literature review. Ingénierie des systèmes d information. 2023; 28(6): 1701–1708. doi: 10.18280/isi.280629
74. Kienberger S, Lang S, Zeil P. Spatial vulnerability units–expert-based spatial modelling of socio-economic vulnerability in the Salzach catchment, Austria. Natural Hazards and Earth System Sciences. 2009; 9(3): 767–778. doi: 10.5194/nhess-9-767-2009
75. Malczewski J. GIS-based multicriteria decision analysis: a survey of the literature. International Journal of Geographical Information Science. 2006; 20(7): 703–726. doi: 10.1080/13658810600661508
76. Feizizadeh B, Shadman Roodposhti M, Jankowski P, et al. A GIS-based extended fuzzy multi-criteria evaluation for landslide susceptibility mapping. Computers & Geosciences. 2014; 73: 208–221. doi: 10.1016/j.cageo.2014.08.001
77. Merz B, Kreibich H, Schwarze R, et al. Review Article " Assessment of Economic Flood Damage & quot; Nat. Hazards and Earth System Science. 2010; 10: 1697–1724. doi: 10.5194/nhess-10-1697-2010
78. Rehman A, Song J, Haq F, et al. Multi-Hazard susceptibility assessment using the analytical hierarchy process and frequency ratio techniques in the northwest himalayas, Pakistan. Remote Sensing. 2022; 14(3): 554. doi: 10.3390/rs14030554
79. Halder B, Barman S, Banik P, et al. Large-scale flood hazard monitoring and impact assessment on landscape: Representative case study in India. Sustainability. 2023; 15(14): 11413. doi: 10.3390/su151411413